Eur. Phys. J. B **25**, 313–317 (2002)
DOI: 10.1140/epjb/e20020036

THE EUROPEAN PHYSICAL JOURNAL B
EDP Sciences

Transition to plastic motion as a critical phenomenon and anomalous interface layer of a 2D driven vortex lattice

L. Fruchter[a]

Laboratoire de Physique des Solides, CNRS Université Paris-Sud, 91405 Orsay Cedex, France

Received 22 September 2001

Abstract. The dynamic transition between ordered flow and plastic flow is studied for a two-dimensional driven vortex lattice, in the presence of sharp and dense pinning centers, from numerical simulations. For this system, which does not show smectic ordering, the lattice exhibits a first order transition from a crystal to a liquid, shortly followed by the dynamical transition to plastic flow. The resistivity provides a critical order parameter for the latter, and critical exponents are determined in analogy with a percolation transition. At the boundary between a pinned region and an unpinned one, an anomalous layer is observed, where the vortices are more strongly pinned than in the bulk.

PACS. 64.60.Ht Dynamic critical phenomena – 74.60.Ge Flux pinning, flux creep and flux-line lattice dynamics

1 Introduction

Following extensive studies on the effect of disorder on the static vortex lattice, the physics of the vortex lattice with random quenched disorder and driven by a uniform force has recently attracted much attention. Interacting systems, forming periodic structures at equilibrium, were already the subject of much interest since the earlier studies of charge density waves [1,2]. The complexity of the depinning phenomenon was soon pointed out, in the sense that the description of the depinning threshold by a critical phenomena is no longer valid when one takes into account the possibility of topological defects within the periodic structure [2,3]. Plasticity, which is commonly observed closed to the depinning threshold, is a dramatic illustration in the case of the two dimensional vortex lattice. There have been several investigations of the driven vortex "phase diagram" which have enriched the canonical description [4]: *pinned vortex glass - plastic flow - moving crystal* as the driving force is increased. Amongst these, numerical simulations of two dimensional vortex assemblies, initiated by the work of Brandt [5], have very often accompanied theoretical progress on the subject. After the proliferation of lattice defects was put into evidence, suggesting a dynamic first order melting transition at the occurrence of plastic flow [4,6], numerical simulations [7–9] pointed out the existence at higher drive and for a soft lattice of a moving anisotropic solid with a finite transverse critical force, identified as a smectic state (with transverse periodicity and liquid longitudinal order) from theoretical arguments in reference [10]. Recently, Kolton *et al.* introduced a "frozen transverse solid" beyond this smectic regime, characterized by a drop of the Hall noise [11]. In a general way, there is often some confusion about the exact nature of the "transition". "Dynamical transition" and "phase" are often employed in place of "crossover" or "dynamic regime", without further justification. Indeed, there seems to be up to now only one strong suggestion of a genuine dynamical transition in the works in references [4] and [8]. The fact that the notion of dynamical transition is itself defined only with difficulty (see Ref. [2]) has certainly contributed to this situation. It is not clear, for instance, whether one should try to use some dynamical quantity – such as the correlation length of the local velocities – as was done in reference [2], or if one should use some instantaneous, topological one – such as the concentration of defects or the hexatic order parameter in references [4] and [8] – in the search for an order parameter. Here, it is shown that a simple system, not showing any intermediate smectic order between the ordered and the plastic flow, exhibits a second order like transition to the plastic regime.

2 Experimental details

A two dimensional lattice subjected to a uniform driving force (applied along the y-axis, hereafter denoted longitudinal direction) in the presence of pins is simulated, using the force equation:

$$\mathbf{f_{vv}}(r) + \mathbf{f_p}(r) + \mathbf{f_{B_0}}(x) + \mathbf{J} \wedge \Phi_\mathbf{0} - \eta\, \dot{\mathbf{r}} = 0. \qquad (1)$$

The geometry is analogous to the one of a Corbino disk experiment: the two edges at y = const. are subjected

[a] e-mail: fruchter@lps.u-psud.fr

to a periodic boundary condition; the ones at $x = \text{const.}$ are subjected to an external magnetic field, B_0, which is simulated by an extra force f_{B_0} acting on each vortex, perpendicular to the edges. The force, $f_{B_0}(x)$, acting on a vortex at a distance x from the edge, is that imposed by a semi-infinite vortex lattice at a distance $a_0 + x$, where $a_0 = (\Phi_0/B)^{1/2}$ is the flux lattice spacing at equilibrium. Flux lines are assumed rigid rods and the force per unit length between vortices separated by a distance r is [13]:

$$f_{vv}(r) = (A_V/\lambda)\, K_1\,(r/\lambda) \tag{2}$$

where K_1 is a Bessel function. This is strictly a good approximation only in the case of vortex lines (rods) and for 2D vortices a logarithmic interaction should be used. The interaction between vortices was cut at a distance 5λ, using an interpolation to zero. This was done in order to avoid spurious distortions of the equilibrium lattice from the Abrikosov lattice or the introduction of topological defects, as was shown to occur for a sharp cutoff in reference [14].

The sample dimensions were $100\, a_0$ along x-axis and $70\, a_0$ along y-axis. Strong pinning centers are randomly distributed in the sample. A pin free region was left for $x < 25\, a_0$ and $x > 75\, a_0$. Doing so, a defect free lattice is obtained at the edges of the sample, providing well defined boundary conditions. The density of the pinning sites is $n_{\rm P} = B_\Phi/\Phi_0$, with Φ_0 the flux quantum and B_Φ the "matching field" for which an equilibrium flux line lattice shows the density of flux lines $n_{\rm V} = n_{\rm P}$. The force per unit length exerted by a pin at a distance r from the line is given by:

$$f_p(r) = (2\, A_{\rm P}/r_{\rm P})\ (r/r_{\rm P});\ \text{for } r \le r_{\rm P},\ 0 \text{ for } r > r_{\rm P}. \tag{3}$$

The pinning force is exactly balanced by the Lorentz force, $\mathbf{J} \wedge \boldsymbol{\Phi_0}$, for $J = J_0 = 2\, A_{\rm V}/r_{\rm P}\ \Phi_0$ (in the following, $j = J/J_0$). In the present study, the following parameters were used: $\lambda = 1.57\, a_0$, $r_{\rm P} = 4.9\times10^{-2}\, a_0$, $A_{\rm P}/A_{\rm V} = 2.5\times10^{-2}$ and $B_\Phi = 6\, B$. Using the notations in [5], this corresponds to sharp, dense and strong ($A_{\rm P}/r_0\ a_0\ c_{66} \gg 1$) pins. The sample contained approximately $N_{\rm V} = 7000$ vortices and 25 000 pins.

3 Results and discussion

Vortices trajectories are shown in Figure 1. At first sight, they display a striking feature: as the driving current decreases and the trajectories evolve from correlated channels to branched trajectories, the vortices are first pinned at the interfaces between the pinned and the unpinned region. This is in contradiction with the intuition gained from fluid dynamics physics, where one would expect the average velocity of the fluid to decrease monotonically from the one for unpinned vortices to the one of vortices slowed down by solid friction. Rather, as shown in Figure 2, the average velocity first drops to a minimum right at the interface between the pinned and the unpinned region, and then grows to some roughly uniform value at

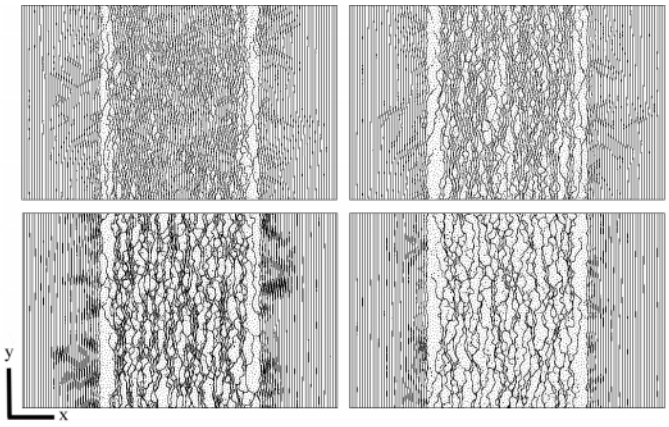

Fig. 1. Vortices trajectories under uniform driving current density applied along x-axis. Top left and right: $j = 0.31$ and 0.295, bottom: 0.27 and 0.24.

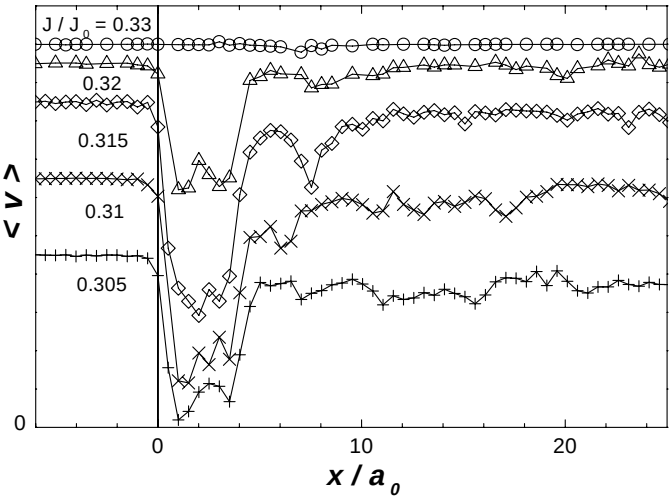

Fig. 2. Average y-velocity component profile. The pinning center density is non zero where $x \ge 0$. For clarity, results for each curve were rescaled along the vertical axis.

a distance $\approx 5\, a_0$ from the interface. The magnitude of this anomalous boundary layer effect may be measured as the ratio of the average velocity in the layer, to the one far away in the pinned region (Fig. 3c). Dynamics regimes were characterized using physical quantities as commonly done in flux lattice simulations [7,9,11]. As shown in Figure 3, the system exhibits a sharp departure from a linear $V - I$ characteristic; an onset of the voltage noise measured in the direction transverse to the average flux flow; an onset of the lattice diffraction peaks widening as well as the onset of the anomalous layer effect at $j_1 \simeq 0.33$. Close to this value, at $j_2 \simeq 0.305$, the voltage derivative, $\mathrm{d}V/\mathrm{d}J$, shows a sharp peak; diffraction peaks vanish and the layer effect saturates. The analysis of the structure factor $S(\mathbf{k}) = n_{\rm V}^{-1}\ |\sum_i \mathrm{e}^{\mathrm{i}\,\mathbf{k}\,\mathbf{r_i}}|^2$ on an annulus which overlaps the first Brillouin zone diffraction peaks (Fig. 4) shows the progressive evolution of the central region of the sample from a well ordered hexagonal lattice at $j = j_1$ to a liquid at j_2. In between, there is no evidence in the diffraction intensity for an asymmetry between the average flux flow

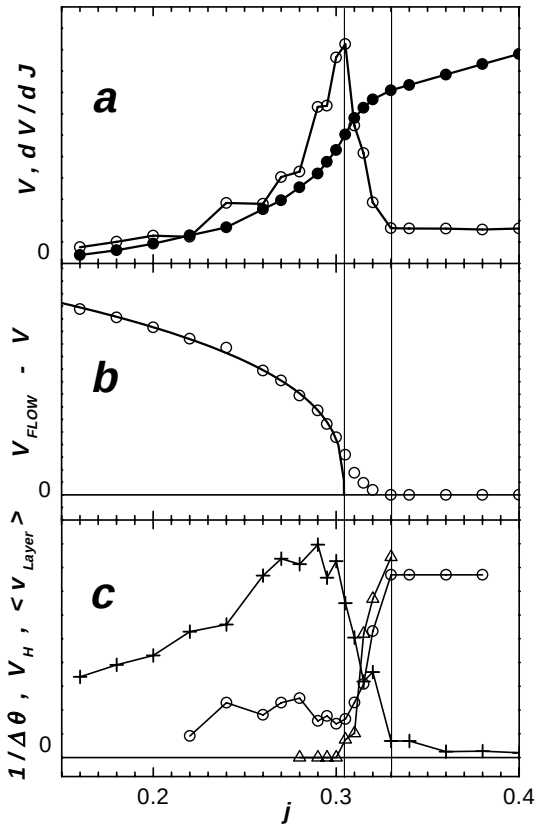

Fig. 3. (a) filled: average voltage along the main flow, computed in the pinned region, away from the anomalous layer; (a) empty: voltage derivative. (b) points: difference between voltage in (a) and the free flux flow voltage; (b) line: fit to $V_0(1-j/j_C)^\beta$, where $j_C = 0.304 \pm 0.001$ and $\beta = 0.34 \pm 0.02$. (c) crosses: transverse Hall noise; (c) circles: average velocity in the anomalous layer, normalized to that of the bulk; (c) triangles: inverse of the width of the diffraction peak at $k = (a_0, 0)$. The vertical line at $j = 0.304$ marks the critical driving current, as given by the fit in (b); the one at $j = 0.33$, the onset of departure from the free flux flow potential in (a).

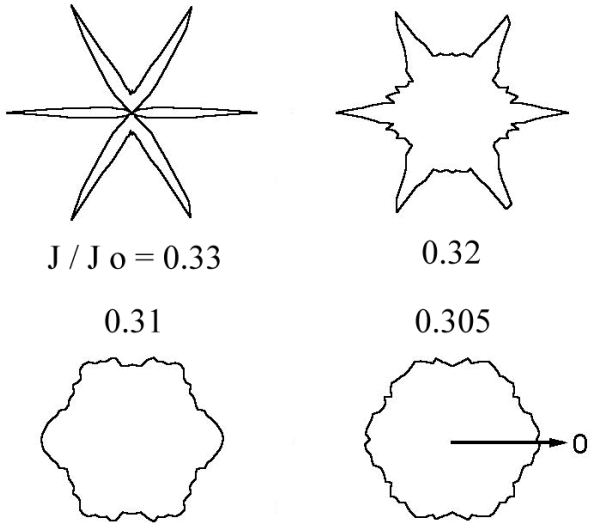

Fig. 4. Polar plot (logarithmic units) of the instantaneous structure factor, after radial integration over an annulus which overlaps the diffraction peaks in the first Brillouin zone (the flux lattice is sampled in the pinned region, away from the anomalous layer). The zero angle axis points along the reciprocal direction transverse to the average flux flow.

direction and the one transverse to it. Following reference [9], the regime at $j \leq j_2$ is that of the plastic flow of the amorphous solid. The transition region $j_2 < j < j_1$ between the plastic regime and the ordered state differs from the ones described in [9] or [11], as we find no evidence for the asymmetry needed in the diffraction intensity for a smectic order or an order intermediate between a smectic and a crystal. Also, the transition regime width observed here is only about 10% of the critical value for the plastic to quasi-ordered regime current, while values larger than 30% were found in [9]. These differences are due to parameters much different from the ones used in [9]. Here, pinning sites are dense and almost point like ($n_P/n_V = 6$ and $a_0/r_P = 25$), while the pinning density is comparable to the vortex density and pinning sites are extended in [9] ($n_P/n_V = 1.4$ and $ab/r_P = 4$). As a result, vortices do not sense here the asymmetry of the pinning potential (when it is tilted by the driving force) as they do for extended defects, and the smectic regime does not occur.

Within the plastic regime, the evolution of the channels resembles that of a percolation transition, and the transition between the ordered flow and the plastic regime may be viewed as the percolation of dynamic flux channels in the transverse direction. This similarity was already noticed earlier in [8]. The analysis of the resistivity quantitatively demonstrates the validity of a critical phenomenon approach. As seen in Figure 3b, the resistivity may be fitted to a critical order parameter of the form $(1-j/j_C)^\beta$, with $\beta = 0.34 \pm 0.02$. The critical driving force obtained in this way, j_C, is within fitting uncertainty identical to j_2. The restricted intermediate regime, as observed here, might be crucial for the observation of the critical behavior, as it tends to smear out the transition. The interpretation of the anomalous layer effect – which is fully developed once one has entered the plastic dynamical phase (as defined from the critical analysis above) – appeals for a better understanding of the latter. Characterization of the instantaneous structure, such as the structure factor displayed above, is useless to the study of the plastic phase: the autocorrelation function of the instantaneous vortices positions, $\mathcal{C}(\mathbf{k}) = \langle \rho(\mathbf{r})\, \rho(\mathbf{r}+\mathbf{k}) \rangle_{\mathbf{r}}$, where $\rho(\mathbf{r}) = \sum_{i=1}^{n_V} \delta(\mathbf{r_i})$ only confirms an evidence for a liquid order (Fig. 5). Considering the existence of two distinct vortices populations [15]: a rapidly moving ensemble of vortices along quasi static channels and quasi pinned ones, one may also define the velocity-weighted autocorrelation function, $\mathcal{C}_V(\mathbf{k}) = \langle \rho_V(\mathbf{r})\, \rho_V(\mathbf{r}+\mathbf{k}) \rangle_{\mathbf{r}}$ where $\rho_V(\mathbf{r}) = \sum_{i=1}^{N_V} \delta(\mathbf{r_i})\, \dot{r}_i$. This essentially measures the correlation amongst the most mobile vortices. As can be seen in Figure 5, the function evolves from the one of a liquid to the one characteristic of isolated flux channels (two peaks at $\mathbf{k} = (\pm a_0, 0)$) as j decreases. Both $\mathcal{C}(\mathbf{k})$ and $\mathcal{C}_V(\mathbf{k})$ show that second neighbor correlations are

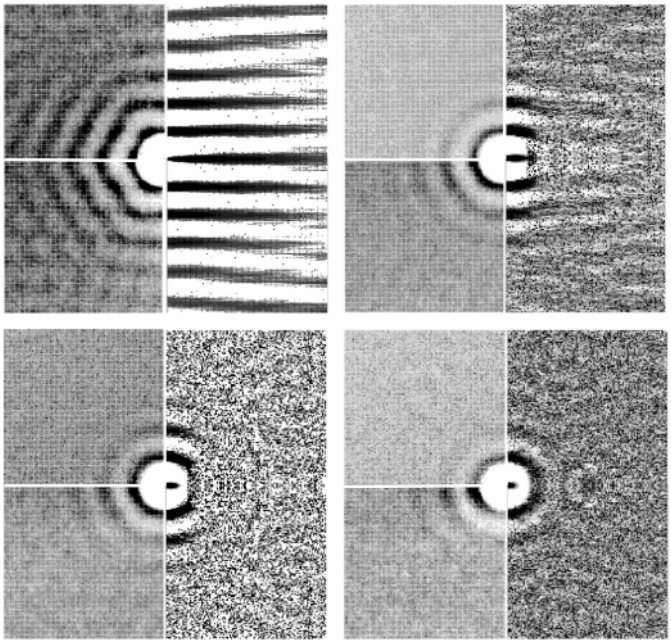

Fig. 5. Gray scale maps of autocorrelation functions. Clockwise: $j = 0.31,\ 0.295,\ 0.27,\ 0.24$. Left upper quadrant: autocorrelation function of the instantaneous lattice, $\mathcal{C}(\mathbf{k})$. Left lower quadrant: autocorrelation function of the instantaneous lattice, weighted by the y-velocity component, $\mathcal{C}_{\mathrm{V}}(\mathbf{k})$. Right half: autocorrelation function of the vortices trajectories, weighted by the y-velocity component, $\mathcal{C}_{\mathrm{C}}(\mathbf{k})$. The average flux flow is horizontal.

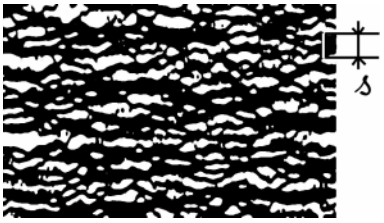

Fig. 6. Channel structure ($j = 0.27$), filtered from frequencies higher than a_0^{-1}. Shown as a white line is a one-dimensional cluster of size s.

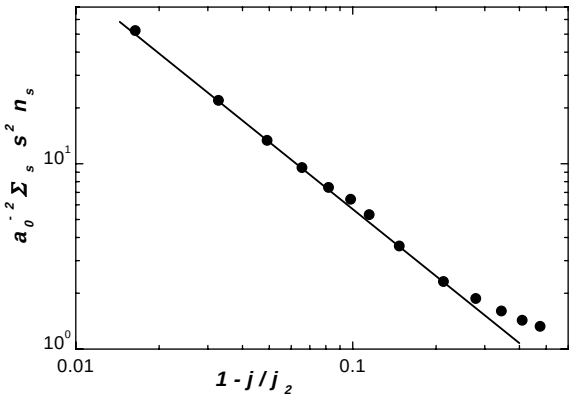

Fig. 7. Mean cluster size, normalized to a_0^2. The line is a fit to $(1 - j/j_2)^{-\gamma}$ with $\gamma = 1.2 \pm 0.02$.

strongly damped in the transverse direction. However, correlations between vortices may be found that are less demanding than the ones uncovered by the transformations of the instantaneous lattice. The autocorrelation function of the channels, defined as: $\mathcal{C}_{\mathrm{C}}(\mathbf{k}) = \langle \rho_t(\mathbf{r})\ \rho_t(\mathbf{r}+\mathbf{k}) \rangle_{\mathbf{r}}$ where $\rho_t(\mathbf{r}) = \int_0^t \rho_{\mathrm{V}}(\mathbf{r})\ \mathrm{d}t$ and t is a time large enough so that the most mobile vortices have moved by a distance larger than a_0, provides evidence – close to the transition – for stronger transverse correlations between such channels than the ones uncovered by $\mathcal{C}(\mathbf{k})$ or $\mathcal{C}_{\mathrm{V}}(\mathbf{k})$ (Fig. 5). This means that channels tend to correlate in the direction transverse to the average flux flow.

The qualitative analogy with percolation and the definition of a critical order parameter, as shown above, both appeal for a definition of dynamic clusters. This is done in the following way: first, $\rho_t(\mathbf{r})$ is computed as defined above, thus providing some snapshots of the channels. Then, the pattern defined in this way is filtered from frequencies larger than a_0^{-1} (this ensures that two contiguous channels do belong to the same cluster). Finally, one-dimensional clusters are defined, as the line segments perpendicular to the average flux flow that are entirely contained within the filtered channels (Fig. 6). Such a definition takes into account the anisotropy of the problem and ensures that an infinite cluster is found at the transition. Although it provides an infinite number of clusters for each sample, it allows the study of cluster distributions as commonly done in the study of percolation [16]. The first infinite cluster is found at $j = j_2$, in agreement with the critical analysis of the resistivity. As shown in Figure 7, it is found that the mean cluster size, $S = \sum_s s^2\ n_s$ scales close to j_2 as $(1-j)^{-\gamma}$ with $\gamma = 1.2 \pm 0.02$. For $j < 0.2$, the mean cluster size saturates to $S = a_0^2$, meaning that one enters a regime of isolated flux channels. This agrees with $\mathcal{C}_{\mathrm{C}}(\mathbf{k})$ in Figure 5, where it is seen that the first neighbor correlation roughly become isotropic below $j \approx 0.2$. Following the analogy with percolation, one may also define a correlation length, ξ, which diverges at j_2. Then, the saturation observed for S may be directly interpreted as the decrease of ξ down to the average flux line spacing, a_0. Within this description, it could be appealing to interpret the existence of the anomalous interface layer as a "proximity effect". However, the order parameter – as defined above – should in this case continuously *increase* from zero in the ordered phase, to the value of the bulk over a distance comparable to ξ, whereas it is anomalously large in the pinned layer. Also, the thickness of the anomalous layer should strongly depend upon j, which is not observed in Figure 2. A more plausible interpretation for the effect is in fact a topological one. The transverse wandering of channels – an alternative view for the cluster distribution and the fractal topology of the plastic phase – is strongly suppressed at the interface with the ordered phase. Besides the occurrence of the ordered phase, the occurrence of a pinned region at the interface provides another way to pin the transverse excursions of the vortices as imposed by the proximity of the crystal structure, hence the observed effect. However, this piece of explanation does not provide any estimation for the width of the layer. This shows that,

although the present analysis provides some evidence for the existence of a dynamical plastic phase and a second order like transition, we still lack a complete understanding for the pinned, driven vortex lattice.

I gratefully acknowledge valuable help from S. Ravy in the handling of numerical diffraction data. The author is grateful to the IDRIS institute for providing computer time on its vectorial computer.

References

1. H. Fukuyama, P.A. Lee, Phys. Rev. B **17**, 535 (1972).
2. D.S. Fisher, Phys. Rev. B **31**, 1396 (1985).
3. S.N. Coppersmith, A.J. Millis, Phys. Rev. B **44**, 7799 (1991).
4. A.E. Koshelev, V.M. Vinokur, Phys. Rev. Lett. **73**, 3580 (1994).
5. E.H. Brandt, Phys. Rev. Lett. **50**, 1599 (1983).
6. U. Yaron, P.L. Gammel, D.A. Huse, R.N. Kleiman, C.S. Oglesby, E. Bucher, B. Batlogg, D.J. Bishop, K. Mortensen, K.N. Clausen, Nature **376**, 753 (1995).
7. K. Moon, R.T. Scalettar, G.T. Zimanyl, Phys. Rev. Lett. **77**, 2778 (1996).
8. R. Seungoh, M. Hellerqvist, S. Doniach, A. Kapitulnik, D. Stroud, Phys. Rev. Lett. **77**, 5114 (1996).
9. C.J. Olson, C. Reichhardt, F. Nori, Phys. Rev. Lett. **81**, 3757 (1998).
10. L. Balents, M.C. Marchetti, L. Radzihovsky, Phys. Rev. Lett. **78**, 751 (1997); T. Giamarchi, P. Le Doussal, Phys. Rev. Lett. **78**, 752 (1997).
11. A.B. Kolton, D. Dominguez, N. Gronbech-Jensen, Phys. Rev. Lett. **83**, 3061 (1999).
12. M. Feigel'man, V. Geshkenbeim, A. Larkin, V. Vinokur, Phys. Rev. Lett. **63**, 2303 (1989).
13. E.H. Brandt, J. Low Temp. Phys. **53**, 41 (1983).
14. H. Fangohr, A.R. Rice, S.J. Cox, P.A.J. de Groot, G.J. Daniell, K.S. Thomas, J. Comput. Phys. **162**, 372 (2000).
15. M.C. Faleski, M.C. Marchetti, A.A. Middleton, Phys. Rev. B **54**, 12427 (1996).
16. D. Stauffer, *Introduction to percolation theory* (Taylor and Francis, 1985).